ELSEVIER

Ceramics International 30 (2004) 213–217

CERAMICS INTERNATIONAL

www.elsevier.com/locate/ceramint

R-curve behavior of laminated SiC/BN ceramics

Dongyun Li*, Guanjun Qiao, Zhihao Jin

State Key Laboratory for Mechanical Behavior of Materials, School of Materials Science and Engineering, Xi'an Jiaotong University, Xi'an 710049, PR China

Received 22 November 2002; received in revised form 7 March 2003; accepted 7 April 2003

Abstract

Laminated SiC/BN ceramics with a perfect layered structure was fabricated by tap-casting process and hot-pressing sintering. Damage resistance and *R*-curve behavior of laminated SiC/BN ceramics were evaluated using the indentation-strength-in-bending technique, and compared with those of monolithic SiC ceramics. The results showed that the indentation strengths for monolithic SiC ceramics decreased steeply with indentation load, while for laminated SiC/BN ceramics reduced slightly with indentation load, suggesting an exceptional damage resistance. Moreover, a rising *R*-curve behavior was demonstrated for laminated SiC/BN ceramics, a plateau *R*-curve behavior for monolithic SiC ceramics. The excellent damage resistance and pronounced *R*-curve behavior of laminated SiC/BN ceramics were attributed to crack deflection, crack branching and crack delamination at the SiC/BN weak interfaces.

Keywords: B. Interface; C. Fracture; C. Mechanical properties; D. SiC

1. Introduction

When ceramic materials are applied to structural components, the lack of damage-tolerance is one of the most crucial problems. Ceramic composites with a layered structure have been considered to offer one of the most important approaches to this problem, and a number of studies have been conducted so far in several systems including alumina/zirconia [1–4], alumina/aluminium titanate [5], mullite/alumina [6], silicon carbide [7–10] and silicon nitride [11–13]. These laminated ceramics have been reported to exhibit increased apparent fracture toughness and fracture energy as well as a non-catastrophic fracture behavior. However, little work has been performed on the flaw tolerance and fracture resistance behavior of the layered ceramics.

Silicon carbon (SiC) layered ceramics with weak boron nitride (BN) interphases have been previously manufactured in a conventional two-dimensional layered structure [14], as well as in microcomposites [15]. For the former, impressive properties were achieved with strengths of ~729 MPa and fracture toughness of ~20.5 MPa $m^{1/2}$. For the latter, damage capability and oxidation resistance were improved in comparison with microcomposites with a carbon interphase. These properties make this system attractive for applications.

In this paper, laminated SiC/BN ceramics (hereafter denoted by LSB) with a perfect layered structure were fabricated by tap-casting process and hot-pressing sintering. Damage resistance and *R*-curve behavior of LSB are evaluated using the indentation-strength-in-bending technique (ISB), and compared with those of monolithic SiC ceramics (hereafter MS), the difference between the two being analyzed.

2. Experimental procedure

2.1. Materials

The flow chart for the fabrication process of LSB is shown in Fig. 1. Briefly, submicrometer silicon carbide powders with sintering additives 6 wt.% alumina and 4 wt.% yttria and the organic additives were mixed and cast into the green tapes, then coated with BN-containing

* Corresponding author. Tel.: +86-29-266-7942; fax: +86-29-266-5443.

E-mail address: dongyun_li@hotmail.com (D. Li).

0272-8842/03/$30.00
doi:10.1016/S0272-8842(03)00091-9

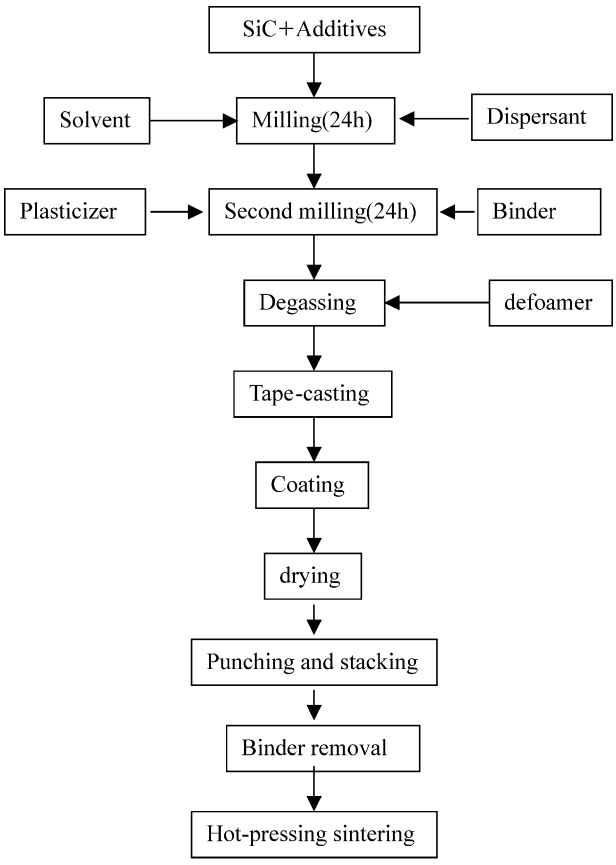

Fig. 1. Flow chart of fabrication process of LSB.

slurry. After coating, the green laminates were dried, stacked, and the organic additives were removed. Finally, they were sintered under a 30 MPa pressure at 1850 °C for 1 h in a nitrogen atmosphere. The obtained layered structure is shown in Fig. 2. As can be seen, the SiC layers (dark regions) and BN (gray regions) are reasonably uniform and the interfaces are straight and well-distinguishable. For comparison, MS were fabricated by stacking SiC green tapes without BN coating using the same fabrication process as for LSB.

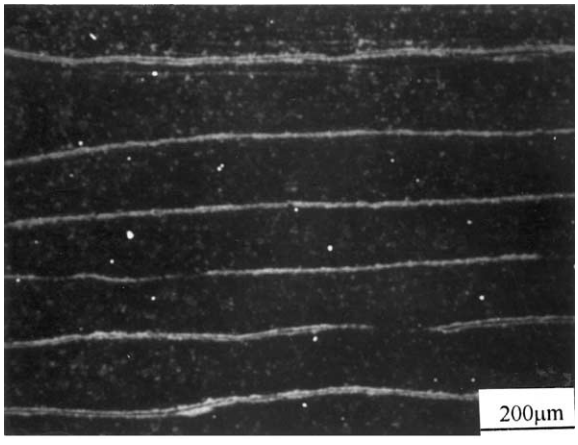

Fig. 2. SEM micrograph of the cross section of LSB.

2.2. ISB test

To evaluate damage resistance and *R*-curve behavior, the hot-pressed billets of both LSB and MS were cut and ground into rectangular specimens; the prospective tensile surfaces of the specimens were perpendicular to the hot-pressing direction, normal to the layer plane. The nominal dimensions of the test specimens were 3×4×30 mm. The test specimens were indented at the center of the polished prospective tensile surface (4-mm-wide side) using a Vickers diamond pyramid indenter under loads ranging from 0.1 to 300 N. Care was taken to orient one set of the indentation cracks to be parallel to the longitudinal axis of the rectangular specimens. After indentation, the specimens were tested in three-point bending with a span of 24 mm and a crosshead speed of 0.5 mm/min (Testing machine: instron 1195). Four tests were performed for each indentation load.

Conversion of Vickers ISB data σ_f (P), to generate a toughness curve, $T(c)$ [$T(c)=K_R$] is as follows [16]. Conversion is accomplished using an objective indentation-strength K-field analysis. Under the action of applied stress σ_A, radial cracks of size c produced at an indentation load P extend according to the equilibrium condition,

$$K'_A(c) = \psi\sigma_A c^{1/2} + \chi P c^{-3/2} = T(c) \quad (1)$$

where $K'_A(c)$ is a global applied stress intensity factor corresponding to an applied stress σ_A, $T(c)$ the toughness curve, and ψ the crack shape factor which depends on crack and specimen geometry. χ the residual contact coefficient which is often expressed in terms of Young's modulus E and hardness H [17],$\chi = \xi(E/H)^{1/2}$ ξ being a factor of proportionality equals to 0.016 [18]. The value of E/H can be measured by the Knoop indentation method proposed by Marshall et al. [19].

For a given indentation load P, failure occurs at that applied stress $\sigma_A=\sigma_f$ which satisfies the "tangency condition",

$$dK'_A(c)/dc = dT(c)/dc \quad (3)$$

Accordingly, given an appropriate calibration of the coefficients ψ and χ, families of $K'_A(c)$ curves can be generated from the $\sigma_f(P)$ data. $T(c)$ then can be determined objectively as envelopes of tangency points to these families of curves [16].

3. Results and discussion

3.1. Load–displacement curves

Fig. 3 shows the load–displacement curves of the indented specimens for LSB and MS. Evidently, the fracture behavior of LSB was quite different from that of MS. MS fractured catastrophically, while LSB

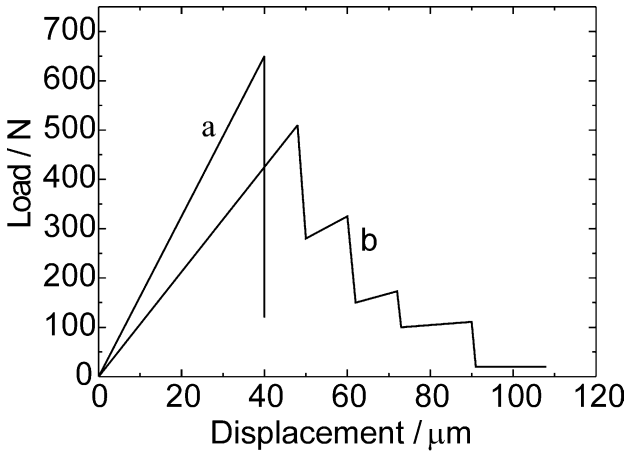

Fig. 3. Load–displacement curves of the two types of specimens with an indentation in the tensile surface: (a) MS, (b) LSB.

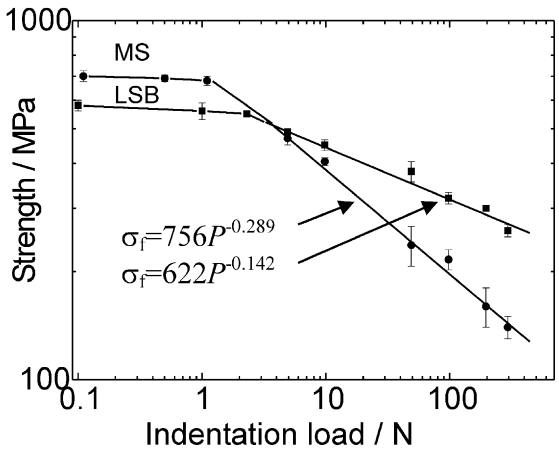

Fig. 5. Strength plotted against indentation load for the two materials. Curves for the two materials deviate slightly from slope of −1/3.

showed a progressive failure behavior. Upon initial loading, LSB also deformed in a linear elastic fashion until the crack reached the same stress intensity as MS. However, rather than traveling right across the specimen the crack was deflected at the first BN interface that it reached, as shown in Fig. 4. Crack deflection along the weak interface allowed the load to continue rising. Failure of the second SiC layer gave rise to the first load drop. This process was repeated until all the SiC layers had cracked, resulting in a step-like load–displacement response. The total area under the load–displacement curve represented the work-of-fracture (WOF). Evidently, WOF of LSB was much higher than that of MS

3.2. *Indentation strengths and* R-*curves*

Indentation fracture strength, σ_f, is plotted logarithmically against indentation load, P, in Fig. 5 for both MS and LSB. For each of the two materials a knee in the corresponding curve (at $P = P^*$) separated the plot in Fig. 5 into two regions. In the left region, for specimens with a low indentation load, the strength was not load-dependent, because it was microstructure-controlled. On the other hand, in the right region, where specimens had a higher indentation load, strength was inversely related to the indentation load, because strength was controlled by external flaws.

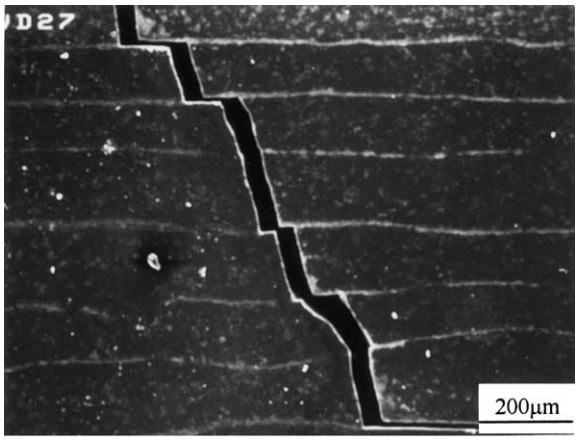

Fig. 4. Propagation of a major crack through the specimen of LSB. Note that crack deflection occurs along the SiC/BN interfaces.

Fig. 5 shows that in the low-indentation-load region the strengths were higher for MS than for LSB, in the high-indentation-load region the strengths for the two materials decreased linearly with indentation load, but the slope being much steeper for MS than for LSB. This means that LSB have a higher retained strength than MS for an equivalent indentation load, hence an improved damage tolerance in comparison with MS. It also suggested that LSB might have a higher fracture resistance than MS.

R-curves of two materials were obtained from indentation-strength data. Linear regression was used to obtain the best fit for the experimental data in Fig. 5. It showed that the slopes of MS and LSB were −0.289 and −0.142, respectively. Griffith materials, for which the R-curve is flat, would follow the power law, $\sigma_f \propto P^{-k}$ with $k = 1/3$. The fact that k is lower than 1/3, suggests a rising R-curve behavior for both materials. If the Vickers crack geometry is considered to be material-independent, the values $\psi = 1.24$ [20], $\chi = 0.071$ can be calculated for the experimental value $E/H = 20$ for MS. we use the same values of ψ and χ for the two materials. Two families of $K'_A(c)$ curves can now be constructed from the indentation-strength data in Fig. 5, inserting $\sigma_A = \sigma_f$ at each value of indentation load P in Eq. (1). The envelopes of tangency points for two materials are shown in Fig. 6. It can be seen from Fig. 6 that the envelope of tangency points for MS was approximately horizontal, indicative of a plateau R-curve behavior, while, for LSB the envelope of tangency points yields a rising R-curve. This suggests that LSB possessed excellent

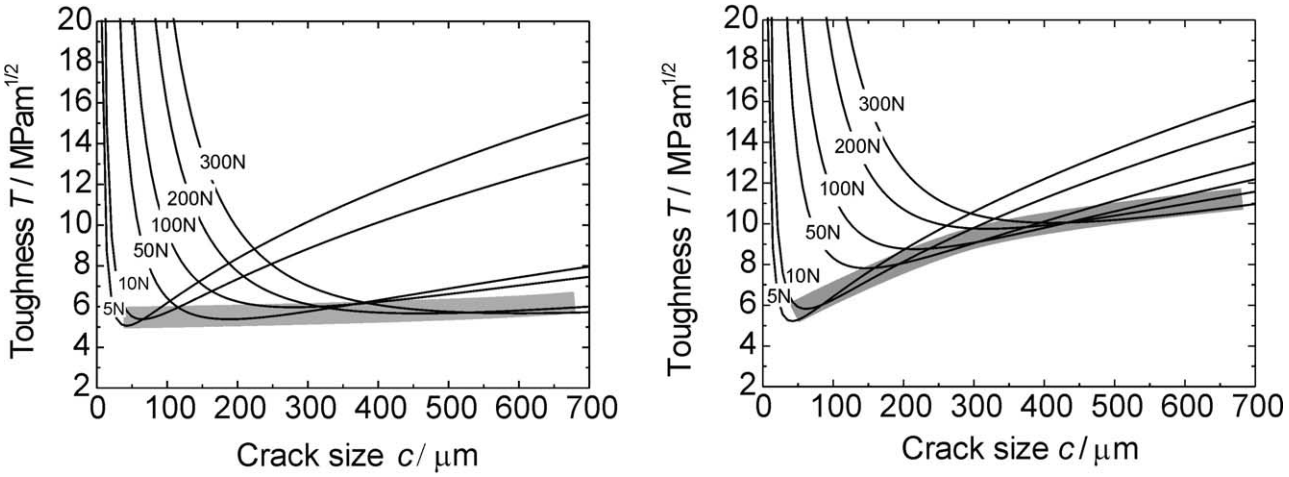

Fig. 6. Toughness curve diagrams for (a) MS, (b) LSB. Families of solid curves are plots of $K'_A(c)$ in Eq. (1) using strength data in Fig. 5. Shaded lines are $T(c)$ functions, plotted as locus of tangency points to $K'_A(c)$.

damage tolerance and a rising *R*-curve behavior in comparison with MS.

3.3. The main toughening mechanisms

The above results showed that LSB possessed excellent damage tolerance and a rising *R*-curve behavior in comparison with MS. This was thought be related to their different toughening mechanisms. Fig. 7 showed the crack propagation path of MS, which introduced by Vickers indentation, crack deflection along weak grain interface is its main toughening mechanism. The main toughening mechanism of LSB is crack deflection along weak BN interface continually. As shown in Fig. 4, when a crack propagates through LSB, crack deflection occurred along weak interface continually, leading to a step-like crack propagation path which greatly extended effective crack length and absorbed more fracture energy, with an improvement of fracture resistance. Besides, crack branching and crack delamination which appeared at the weak interface, as shown in Fig. 8, further absorbed the fracture energy of materials, relaxed the stress at the crack tip and improved the fracture resistance and damage resistance.

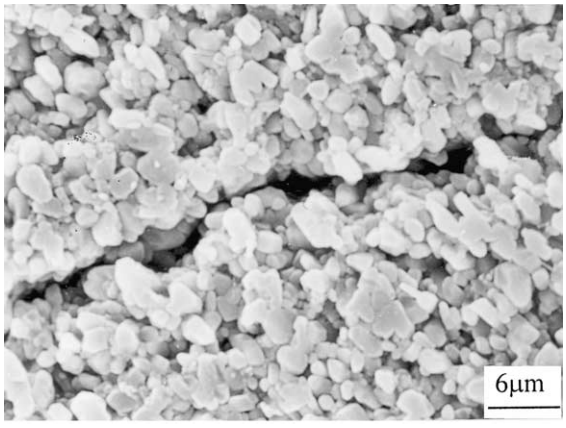

Fig. 7. Crack propagation path of MS.

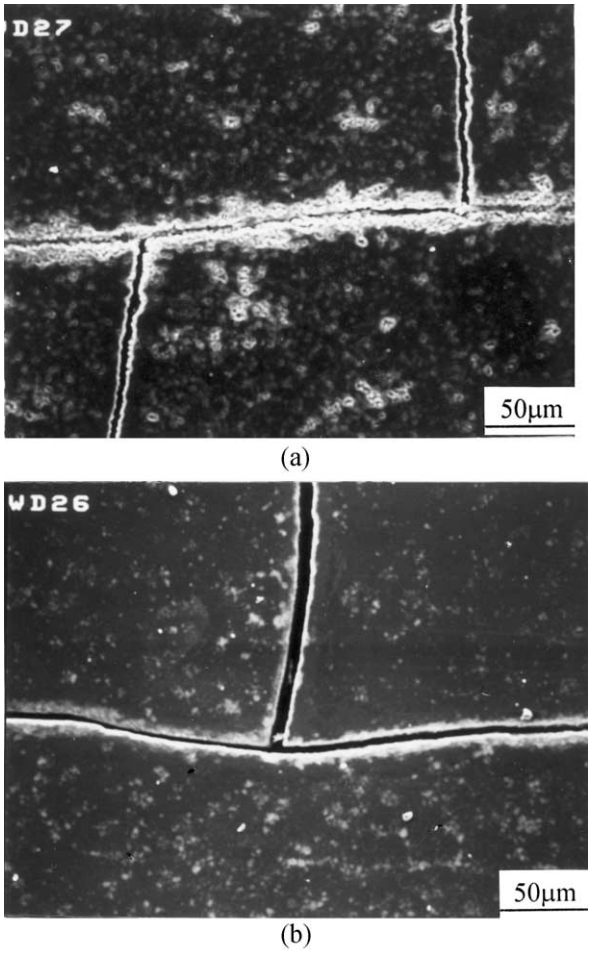

Fig. 8. Two cracking mode of LSB for (a) crack branching, (b) crack delamination.

4. Conclusion

The fracture behavior of LSB was quite different from that of MS. MS fractured catastrophically, while LSB showed a non-catastrophic failure behavior. Due to the deflection, branching and delamination of the transverse cracks at the SiC/BN interfaces, the indentation strengths of LSB were observed to be insensitive to the increases in the indentation load, indicative of excellent damage resistance, compared with MS. Furthermore, a rising *R*-curve behavior was demonstrated from ISB test.

Acknowledgements

The authors wish to acknowledge State Key Laboratory for Mechanical Behavior of Materials for financial and technical support.

References

[1] P. Sarkar, X. Haung, P.S. Nicholson, Structural ceramic microlaminates by electrophoretic deposition, J. Am. Ceram. Soc. 75 (10) (1992) 2907–2909.
[2] D.B. Marshall, J.J. Ratto, F.F. Lange, Enhanced fracture toughness in layered microcomposites of Ce-ZrO_2 and Al_2O_3, J. Am. Ceram. Soc. 74 (12) (1991) 2979–2987.
[3] J. Requena, R. Moreno, J.S. Moya, Alumina and alumina/zirconia multilayer composites obtained by slip casting, J. Am. Ceram. Soc. 72 (8) (1989) 1511–1513.
[4] K.P. Plucknett, C.H. Caceres, C. Hughers, D.S. Wilkinson, Processing of tape-cast laminates prepared from fine alumina/zirconia powders, J. Am. Ceram. Soc. 77 (8) (1994) 2145–2153.
[5] C.J. Russo, M.P. Harmer, H.M. Chan, G.A. Miller, Design of laminated ceramic composite for improved strength and toughness, J. Am. Ceram. Soc. 75 (12) (1992) 3396–3400.
[6] H. Katsuki, Y. Hirata, Coat of alumina sheet with needle-like mullite, J. Ceram. Soc. Jpn. 98 (1990) 1114–1119.
[7] J. She, T. Inoue, K. Ueno, Multilayer Al2O3/SiC ceramics with improved mechanical behavior, Ceram. Int. 20 (2000) 1771–1775.
[8] N.P. Padture, D.C. Pender, S. Wuttiphan, B.R. Lawn, In situ processing of silicon carbide layer structures, J. Am. Ceram. Soc. 78 (11) (1995) 3160–3162.
[9] W.J. Clegg, K. Kendall, N.M. Alford, A simple way to make tough ceramics, Nature (London) 347 (1990) 455–461.
[10] W.J. Clegg, The fabrication and failure of laminar ceramic composites, Acta Metall. Mater. 40 (11) (1992) 3085–3093.
[11] H. Liu, B.R. Lawn, S.M. Hsu, Hertzian contact response of tailored silicon nitride multilayers, J. Am. Ceram. Soc. 79 (4) (1996) 1009.
[12] H. Liu, S.M. Hsu, Fracture behavior of multilayer silicon nitride/boron nitride ceramics, J. Am. Ceram. Soc. 79 (9) (1996) 2452–2457.
[13] T. Ohji, Y. Shigegaki, T. Miyajima, Fracture resistance behavior of multilayered silicon nitride, J. Am. Ceram. Soc. 80 (4) (1997) 991–994.
[14] G.J. Yuan, Y.M. Luo, D.M. Chen, Selection of interfacial layer of laminated silicon carbide matrix composites, J. Chinese Ceram. Soc. 29 (3) (2001) 226–231 (in Chinese).
[15] F. Rebillat, A. Guette, L. Espitalier, Oxidation resistance of SiC/SiC micro and minicomposites with a highly crystallised Bn interphase, J. Eur. Ceram. Soc. 18 (1998) 1809–1819.
[16] S.K. Lee, S. Wuttiphan, C.J. Fairbanks, Role of microstructure-strength properties in ceramics: I, effect of crack size on toughness, J. Am. Ceram. Soc. 80 (9) (1997) 2367–2381.
[17] R.F. Cook, Direct observation and analysis of indentation cracking in glass and ceramics, J. Am. Ceram. Soc. 73 (1990) 787–817.
[18] G.T. Antis, A critical evaluation of indentation techniques for measuring fracture toughness-direct crack measurements, J. Am. Ceram. Soc. 64 (2) (1981) 533.
[19] D.B. Marshall, T. Noma, A.G. Evans, A simple method for determining elastic-modulus-to-hardness ratios using Knoop indentation measurements, J. Am. Ceram. Soc. 65 (10) (1982) 175–176.
[20] R.F. Cook, Microstructure–strength properties in ceramics: effect of crack size on toughness, J. Am. Ceram. Soc. 68 (11) (1985) 604–615.